Advances in Colloid and Interface Science 208 (2014) 14–24

Contents lists available at ScienceDirect

Advances in Colloid and Interface Science

journal homepage: www.elsevier.com/locate/cis

Coupling of bending and stretching deformations in vesicle membranes ☆

Reinhard Lipowsky *

Theory and Bio-Systems, Max Planck Institute of Colloids and Interfaces, Science Park Golm, 14424 Potsdam, Germany

ARTICLE INFO

Available online 18 February 2014

Keywords:
Membranes and vesicles
Curvature elasticity
Spontaneous curvature
Compressible membranes
Mechanical tension

ABSTRACT

Biomimetic membranes are fluid and can undergo two different elastic deformations, bending and stretching. The bending of a membrane is primarily governed by two elastic parameters: its spontaneous (or preferred) curvature m and its bending rigidity κ. These two parameters define an intrinsic tension scale, the spontaneous tension $2\kappa m^2$. Membrane stretching and compression, on the other hand, are determined by the mechanical tension acting within the membrane. For vesicle membranes, the two elastic deformations are coupled via the enclosed vesicle volume even in the absence of mechanical forces as shown here by minimizing the combined bending and stretching energy with respect to membrane area for fixed vesicle volume. As a consequence, the mechanical tension within a vesicle membrane depends on the spontaneous curvature and on the bending rigidity. This interdependence, which is difficult to grasp intuitively, is then illustrated for a variety of simple vesicle shapes. Depending on the vesicle morphology, the magnitude of the mechanical tension can be comparable to or can be much smaller than the spontaneous tension.

Contents

☆ Dedicated to Wolfgang Helfrich on the occasion of his 80th birthday.

* Corresponding author.
E-mail address: lipowsky@mpikg.mpg.de.

http://dx.doi.org/10.1016/j.cis.2014.02.008

1. Introduction

I first met Wolfgang Helfrich in 1987 when he invited me to give a talk at the Free University Berlin. It was a very interesting visit, both because of our scientific discussions and because of our excursions to the Berlin wall at the Glienecker Brücke and around Steinstücken. In the following decade, we had many more, highly stimulating discussions on membranes and vesicles. One of the controversial topics at the time was the unbinding transition of interacting membranes [1,2]. Another recurrent theme of our discussions was the notion of 'membrane tension'. This notion is confusing because such a tension can be defined in different ways and one would like to know whether these different definitions lead to the same or to different tensions.

From a mechanical point of view, membrane tension is intimately related to membrane stretching. In his pioneering paper from 1973 [3], Helfrich briefly discussed the stretching of membranes but then argued that one can ignore this elastic deformation compared to the membranes' curvature elasticity. A few years later, Deuling and Helfrich [4] regarded the vesicle membranes as (essentially) incompressible and viewed the tension as a Lagrange multiplier conjugate to the fixed membrane area. The latter viewpoint has been very useful in order to develop quantitative theories for the observed polymorphism of lipid vesicles, see Fig. 1. [5–9].

Additional insight into the notion of membrane tension has been obtained from molecular dynamics simulations. Indeed, in these simulations, one can directly 'measure' the *mechanical tension* of the membranes by calculating their stress (or pressure) profiles [10,11]. In addition, the mechanical tension can be controlled by varying the projected area of the lipid molecules. One then finds an optimal packing of these molecules, for which the mechanical tension vanishes. The latter states represent the natural reference states of the bilayer membranes, see, e.g., [12–17], and our original algorithm for the stress profile [10] has been implemented in popular molecular dynamics packages such as GROMACS.

In the present paper, I will reconsider the mechanical tension within vesicle membranes by minimizing the combined bending and stretching energy of these membranes. This minimization is performed in two steps. First, the vesicle membranes are considered to be incompressible as in the conventional approach introduced by Deuling and Helfrich. One then obtains equilibrium shapes that depend on the vesicle volume, the membrane area, and the parameters of the membrane's bending energy. Second, the area compressibility of the vesicle membranes is taken into account by minimizing the combined bending and stretching energy with respect to membrane area for fixed vesicle volume. As a result, the Lagrange multiplier used to ensure a certain, fixed membrane area in the conventional minimization procedure of the bending energy is found to be identical with the mechanical tension within the vesicle membrane.

The identity of Lagrange multiplier and mechanical tension applies to any form of the bending energy. In order to explicitly calculate the mechanical tension for some simple shapes, I will use the spontaneous curvature model [3,6] because it represents the simplest form of the bending energy and depends only on two elastic parameters, the spontaneous curvature m and the bending rigidity κ. These two parameters define an intrinsic tension scale, the spontaneous tension $2\kappa m^2$ [18,19]. For some vesicle shapes, the mechanical tension is found to be of the order of the spontaneous tension. For other vesicle shapes, the mechanical tension turns out to be much smaller than the spontaneous tension.

The paper is organized as follows. Section 2 reviews some general aspects of curvature elasticity. As shown by molecular dynamics simulations, the concept of curvature applies to membrane patches with a lateral extension that is somewhat larger than the membrane thickness. Therefore, membrane curvature should be viewed as a collective property of many amphiphilic or amphipathic molecules. On nanoscopic or mesoscopic length scales, the bending energy of the membrane can be parametrized in terms of a few elastic parameters. One of these parameters is the spontaneous curvature, which describes possible asymmetries between the two sides of the membranes and can arise from a variety of molecular mechanisms such as the adsorption of ions, small molecules, or proteins. Section 3 describes the conventional approach to determine the shape of vesicles by minimizing the bending energy for fixed vesicle volume and membrane area. In Section 4, the two-step procedure for minimizing the combined bending and stretching energy of the membrane is introduced, which leads to the identification of Lagrange multiplier tension and mechanical tension. The stretching of lipid bilayers is characterized by a rather large value of the area compressibility modulus K_A, which makes it possible to set up an expansion in powers of $1/K_A$ as shown in the last subsection of Section 4. The mechanical tension is then calculated for some simple shapes in Section 5. The paper concludes with a summary and an outlook on more complex membrane systems, which involve some extrinsic tension scales, and on open issues related to the interplay of membrane tension and shape fluctuations.

2. Curvature elasticity of membranes

2.1. Membrane curvature on different length scales

Curvature is a mathematical concept of differential geometry, originally developed to characterize the shape of smooth curves and surfaces. Membranes appear to be rather smooth when viewed on the micron scale in the optical microscope, see Fig. 1, but this smoothness does *not* persist to molecular scales. Indeed, because membranes are immersed in liquid water, each membrane molecule is thermally displaced both parallel and perpendicular to the membrane. The

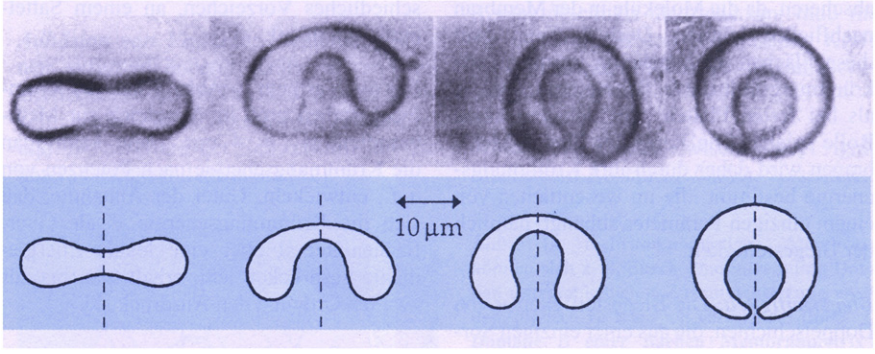

Fig. 1. Different shapes of a giant unilamellar vesicle (top row) are well described by axisymmetric shapes (bottom row) as obtained by minimizing the bending energy of the vesicle membrane. [5].

perpendicular displacements represent molecular protrusions that roughen the two interfaces bounding the membrane, see Fig. 2 [20,21]. Therefore, in order to characterize a lipid/protein bilayer by its curvature, one has to consider small membrane patches and average over the molecular conformations within these patches. The minimal lateral size of these patches can be determined from the analysis of molecular dynamics simulations and was found to be about 1.5 times the membrane thickness, see Fig. 2 [11]. For a lipid bilayer with a thickness of 4 nm, this minimal size is about 6 nm.

A lipid bilayer patch with a lateral size of 6 nm contains about 80 to 100 lipid molecules. Therefore, membrane curvature should be viewed as a supramolecular feature arising from the collective behavior of a large number of membrane molecules. The same conclusion applies to the *spontaneous* curvature of membranes. This curvature describes the intuitive notion that thin layers with two different sides tend to bend or bulge towards one of these sides. This bending or curvature preference was first described by Bancroft for surfactant monolayers in water/oil emulsions [22] and was included by Frank, as the so-called 'splay term', in the curvature elasticity of liquid crystals [23]. In the context of lipid bilayers, spontaneous curvature was first considered by Helfrich [3], who mentioned the analogy with the splay term for liquid crystals.

2.2. Bending energy of curved membranes

We now view the membranes as smooth surfaces with certain elastic properties. The local geometry of these surfaces is then described by their principal curvatures, C_1 and C_2, which define the mean curvature $M = \frac{1}{2}(C_1 + C_2)$ and the Gaussian curvature $G = C_1C_2$. As described in the previous subsection, see Fig. 2, the molecular dynamics simulations imply that such a description applies on nanoscopic scales, for which

$$|M| \lesssim 1/(2\ell_{me}) \tag{1}$$

with a typical value of 4 nm for the membrane thickness ℓ_{me}. The absolute value sign in Eq. (1) is necessary because the mean curvature M can be positive or negative. Here and below, the mean curvature M of a vesicle membrane is taken to be positive and negative when the membrane bulges towards the exterior and interior aqueous compartment, respectively. In Fig. 1, for example, the upper segments of the stomatocyte shapes have a positive curvature whereas the 'interior' segments such as the inverted sphere or spherical in-bud on the rightmost image have a negative curvature.

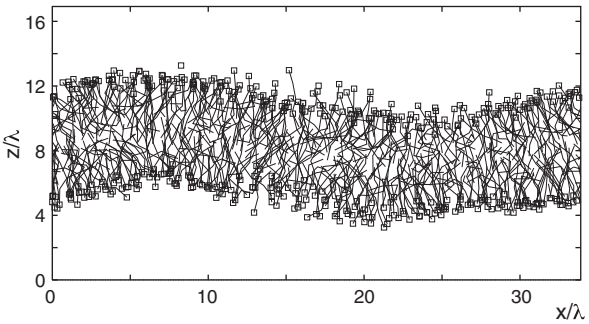

Fig. 2. Typical conformation of a lipid bilayer as observed in molecular dynamics simulations. The bilayer has a thickness of about 4 nm and is bounded by two membrane–water interfaces. These interfaces are roughened by molecular protrusions, which displace the head groups (open squares) perpendicular to the membrane. In order to characterize such a membrane by its curvature, one has to average over membrane segments with a lateral size that exceeds about 1.5 times the bilayer thickness [11].

If the vesicle membrane is asymmetric and does not change its topology, the simplest form of the bending energy for a vesicle of shape $\mathcal{S}$ is given by

$$\mathcal{E}_{be}\{\mathcal{S}\} = \int dA\, 2\kappa (M-m)^2 \tag{2}$$

corresponding to the spontaneous curvature model introduced by Helfrich [3,6]. The notation $E_{be}\{\mathcal{S}\}$ indicates that E_{be} is viewed here as a functional of the vesicle shape $\mathcal{S}$, which is described locally by its mean curvature M. The bending energy (2) depends only on two material parameters, the spontaneous curvature m and the bending rigidity κ.

The bending energy as given by Eq. (2) represents the leading terms of a Taylor expansion in powers of M and G. Higher-order terms of such an expansion have the form

$$\mathcal{E}_{be}^{p,q} \equiv \int dA \kappa_{p,q} M^p G^q \tag{3}$$

where the elastic parameters $\kappa_{p,q}$ have the dimension of energy multiplied by length to the power $p + 2q - 2$. If we take the bending energy κ as the basic energy scale and the membrane thickness ℓ_{me} as the basic molecular length scale, we obtain $\kappa_{p,q} \sim \kappa \ell_{me}^{p+2q-2}$. On the other hand, the basic length scale for the geometric properties of the vesicle shape, such as membrane area, mean curvature, and Gaussian curvature, is provided by the vesicle size R_{ve}. Therefore, dimensional analysis implies that the higher-order terms $\mathcal{E}_{be}^{p,q}$ of the bending energy are proportional to $\kappa (R_{ve}/\ell_{me})^{-(p+2q-2)}$. For large vesicles, i.e., in the limit of large R_{ve}/ℓ_{me}, all terms with $p + 2q > 2$ decay to zero. The term with $p = 0$ and $q = 1$ is special because the integral over G does not depend on the vesicle shape according to the Gauss–Bonnet theorem. Thus, for $R_{ve} \gg \ell_{me}$, the dominant terms correspond to $\mathcal{E}_{be}^{p,0}$ with $0 \le p \le 2$, all of which are contained in the bending energy (2). A systematic classification of the higher-order terms leads to 3 third-order and 8 fourth-order terms [24].

The bending energy (2) represents the area integral over a *local* energy density. In general, the bending of a bilayer membrane consisting of two leaflets may be constrained in a *non-local* manner. Indeed, if the membrane molecules cannot undergo flip-flops between the two leaflets, the number of molecules is fixed within each leaflet and the quenched difference between these two numbers leads to a preferred area difference between the leaflets. This constraint was originally considered by Evans [25], incorporated into the bilayer-coupling model of Svetina and Zeks [26,6], and generalized in terms of the area-difference-elasticity model of Wortis and collaborators [8,9]. However, these constraints on the area difference are expected to become irrelevant if the bilayer membranes contain molecules such as cholesterol that can easily undergo flip-flops and, thus, relax local stresses induced by the bending deformations [27,28].

2.3. Different mechanisms for spontaneous curvature

The molecular bilayer displayed in Fig. 2 is symmetric in the sense that it consists of two leaflets that have the same molecular composition and are exposed to the same aqueous solutions on both sides of the membrane. Real membranes are typically asymmetric. This asymmetry may reflect a variety of different mechanisms such as different molecular compositions of the two leaflets or the insertion of transmembrane molecules with a preferred orientation. In addition, membranes can acquire such an asymmetry from their environment as provided by the exterior and interior aqueous compartments. Indeed, the membranes become asymmetric when these two compartments contain different concentrations of 'particles' such as ions, small molecules, and/or proteins, as indicated in Fig. 3.

One interesting and generic mechanism for the generation of spontaneous curvature is provided by 'particle' adsorption onto the two sides of the membrane [19,30]. Examples are provided by ions [31],

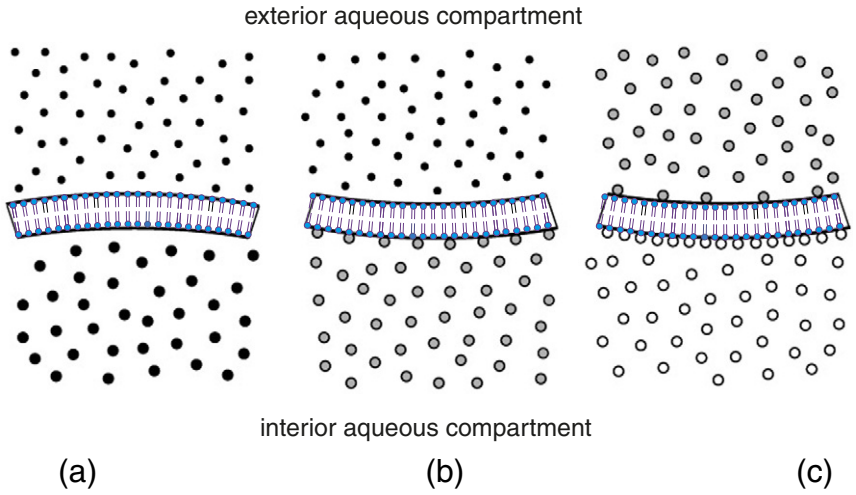

Fig. 3. Spontaneous curvature of membrane segments in contact with different particles such as ions, small molecules, or proteins within the interior and exterior aqueous compartments: (a) Two types of non-adhesive particle species that differ in their size; (b) One adhesive and one non-adhesive species; and (c) Two adhesive species. [29] The spontaneous curvature m induced by the different environments is positive in (a) and negative in (b,c).

small amphipathic peptides [32], or large BAR-domain proteins [33,34]. If these 'particles' have the bulk concentrations Γ_{ex} and Γ_{in} within the exterior and interior aqueous compartments, the adsorption–desorption equilibrium between these compartments and the two membrane/water interfaces will lead to certain adsorbate densities on the two sides of the membrane, even if the membrane contains some lipid components such as cholesterol that undergo relatively fast flip flops. For the sake of simplicity, let us focus here on a single species of adsorbing particles as in Fig. 3(b) and let us ignore the effects of the nonadsorbing species onto the membrane curvature. Energetic considerations then lead to the spontaneous curvature [29,19]

$$m = \frac{k_B T}{4\kappa}\,\ell_{me}(\Gamma_{ex} - \Gamma_{in}) \tag{4}$$

which depends on the thermal energy k_BT, the bending rigidity κ, the membrane thickness ℓ_{me}, and the difference $\Gamma_{ex} - \Gamma_{in}$ of the adsorbate densities on the exterior and interior leaflets. The sign of m follows from the Gibbs adsorption equation, which implies that the membrane bulges towards the leaflet with the higher adsorbate density. Using typical values for these different parameters, the expression (4) leads to the prediction that the spontaneous curvature m induced by the adsorption of small molecules can be quite large with a maximal value of about 1/(20 nm) [19]. The relation (4) between the spontaneous curvature m and the other system parameters has been recently confirmed by coarse-grained molecular dynamics simulations [35].

2.4. Intrinsic tension scale of curvature elasticity

The bending energy as given by Eq. (2) attains its minimal value when the mean curvature M is equal to the spontaneous curvature m everywhere on the membrane surface. The expression (2) also implies that the bending rigidity κ represents a 'spring constant' for deviations of the actual mean curvature M from the spontaneous or preferred curvature m of the membrane.

Real membranes experience a variety of constraints that necessarily lead to such deviations of M from m. One important constraint is provided by the size of the membrane. If the membrane area is large compared to $4\pi/m^2$, the membrane cannot adapt its curvature to the spontaneous curvature by forming a single sphere but can do so by forming a long cylinder with radius $R_{cy} = 1/(2m)$. Another important constraint arises from the osmotic conditions that determine the vesicle volume and, thus, the volume-to-area ratio. If the vesicle volume is increased by osmotic inflation, it will eventually attain a spherical shape with mean curvature $M = 1/R_{sp}$ that usually differs from the spontaneous curvature m of the vesicle membrane. In fact, for a giant spherical vesicle, the actual mean curvature $M = 1/R_{sp}$ can be quite small compared to the spontaneous curvature m and the elastic bending energy of the vesicle membrane is then equal to the membrane area A times the spontaneous tension [19]

$$\sigma \equiv 2\kappa m^2. \tag{5}$$

Such a tension will be present in any membrane segment that has an appreciable spontaneous curvature m but is forced, via external constraints, to assume a mean curvature M that is much smaller than m.

The spontaneous tension σ represents the only tension scale that can be defined by the two elastic parameters κ and m (apart from a dimensionless, multiplicative factor). Therefore, this tension may be viewed as the intrinsic tension scale of curvature elasticity. As shown in Table 1, the spontaneous tension can vary over several orders of magnitude, from very small values of the order of 10^{-8} up to 1 mN/m, the latter value being of the order of the tension of rupture. Depending on the vesicle morphology, the spontaneous tension may or may not provide the scale for the mechanical tension, see Section 5 below.

3. Vesicles with incompressible membranes

In this section, we consider vesicles with incompressible membranes, for which the equilibrium shapes correspond to the minima of the bending energy. The main purpose of this section is to review an explicit relation between the Lagrange multiplier tension used to enforce a certain, fixed membrane area and the bending energy of the (meta)stable vesicle shapes [26,6,38,39] and to provide an intuitive explanation for this relation.

Table 1
Spontaneous (or preferred) curvature m in units of 1/μm and associated spontaneous tension $\sigma = 2\kappa m^2$ in units of 2 mN/m^2 for four different membrane systems where the bending rigidity was taken to have the typical value $\kappa \simeq 10^{-19}$ J.

	Sugar Solutions [36]	DNA Strands [37]	PEG/dextran Solutions [18]	BAR-domain Proteins [33,34]
m [1/μm]	0.01–0.1	0.1–1	3–10	10–50
σ [2 mN/m]	10^{-8}–10^{-6}	10^{-6}–10^{-4}	10^{-3}–10^{-2}	10^{-2}–0.5

3.1. Shape functional for the bending energy

For giant unilamellar vesicles, one can directly measure the vesicle volume V and the membrane area A. Thus, it is rather natural from an experimental point of view to regard V and A as basic control parameters for the vesicle shape. Thus, one would like to minimize the bending energy $\mathcal{E}_{\rm be}\{\mathcal{S}\}$ for fixed V and A, which is conveniently done by introducing two Lagrange multiplier $-\Delta P$ and Σ. Thus, one has to minimize the shape functional

$$\mathcal{E}^{\rm inc}_{\rm ve}\{\mathcal{S}\} = -\Delta P\,\mathcal{V}\{\mathcal{S}\} + \Sigma\,\mathcal{A}\{\mathcal{S}\} + \mathcal{E}_{\rm be}\{\mathcal{S}\}, \tag{6}$$

where the superscript 'inc' refers to incompressible membranes and the curly brackets indicate that $\mathcal{E}^{\rm inc}_{\rm ve}$, $\mathcal{V}$ and $\mathcal{A}$ are functionals of the vesicle shape $\mathcal{S}$. The two Lagrange multipliers have to be chosen in such a way that $\mathcal{V}\{\mathcal{S}\} = V$ and $\mathcal{A}\{\mathcal{S}\} = A$.

The variational problem $\delta\mathcal{E}^{\rm inc}_{\rm ve} = 0$ then leads, in general, to several solutions that form smooth subspaces or 'branches' in the parameter space [6,38]. For each set of parameters, we are primarily interested in those branches that correspond to (meta)stable equilibrium shapes $\mathcal{S}^{\rm eq}$.

3.2. Formal relations for the Lagrange multipliers

In order to get further insight into the two Lagrange multipliers ΔP and Σ, it is useful to change our viewpoint and to regard these two parameters, for the time being, as independent control parameters. The vesicle shapes of each branch are then characterized by the shape energies

$$E^{\rm inc}_{\rm ve}(\Delta P, \Sigma) = \mathcal{E}^{\rm inc}_{\rm ve}\{\mathcal{S}^{\rm eq}\} = -\Delta P V + \Sigma A + \mathcal{E}_{\rm be}\{\mathcal{S}^{\rm eq}\} \tag{7}$$

which implies the relations

$$V = -\left(\frac{dE^{\rm inc}_{\rm ve}}{d\Delta P}\right)_{\Sigma} \tag{8}$$

and

$$A = \left(\frac{dE^{\rm inc}_{\rm ve}}{d\Sigma}\right)_{\Delta P}. \tag{9}$$

Inverting these two relations, we obtain

$$\Delta P = \Delta P(V,A) \quad \text{and} \quad \Sigma = \Sigma(V,A) \tag{10}$$

and the Legendre-transformed shape energy

$$E_{be}(V,A) \equiv E_{\rm ve}(\Delta P, \Sigma) + \Delta P V - \Sigma A = \mathcal{E}_{\rm be}\{\mathcal{S}^{\rm eq}\} \tag{11}$$

which leads to the Lagrange multiplier pressure [26,6,38,39]

$$\Delta P = \left(\frac{dE_{\rm be}(V,A)}{dV}\right)_A \tag{12}$$

and the Lagrange multiplier tension

$$\Sigma = -\left(\frac{dE_{\rm be}(V,A)}{dA}\right)_V. \tag{13}$$

The shape energy $E_{be}(V,A)$ as given by Eq. (11) is physically meaningful and corresponds to the bending energy of a vesicle membrane that encloses the volume V and has the area A. In contrast, the shape energy $E^{\rm inc}_{\rm ve}(\Delta P,\Sigma)$ in Eq. (7) represents an auxiliary quantity that has no direct physical interpretation. In particular, the area term ΣA does *not* correspond to a physical energy and should not be confused with the stretching energy of the membrane as discussed further below.

The relation (13) provides an explicit connection between the Lagrange multiplier tension Σ and the bending energy $E_{\rm be}(V,A)$ along a certain branch of solutions. This relation looks simple but is difficult to grasp intuitively. The vesicle morphology usually involves membrane segments with different curvatures. As we move along a branch of equilibrium shapes by changing the membrane area A for constant vesicle volume V, the area change ΔA is partitioned among these different segments, which can, however, make very different contributions to the bending energy $E_{\rm be}(V,A)$. As an example, consider a vesicle membrane with an appreciable spontaneous curvature m. We can then distinguish weakly curved segments with $|M| \ll |m|$ and strongly curved segments with $M \simeq m$. The area change ΔA is now given by $\Delta A_{wc} + \Delta A_{sc}$, i.e., by the sum of the area changes for the two types of membrane segments. Because the strongly curved segments contribute very little to the bending energy, the change in bending energy is primarily determined by the weakly curved segments and comparable to $2\kappa m^2 \Delta A_{\rm wc} = \sigma \Delta A_{\rm wc}$. Thus, in order to estimate this energy change, we need to know the area decomposition $\Delta A = \Delta A_{wc} + \Delta A_{sc}$, which depends on the vesicle shape and on the vesicle volume V.

4. Vesicles with compressible membranes

In this section, we will include the compressibility of the vesicle membranes and determine their equilibrium shapes by minimizing the combined bending and stretching energy with respect to membrane area for fixed vesicle volume.

4.1. Mechanical tension and stretching energy

In the absence of external forces or constraints, a bilayer membrane attains a certain optimal area $A_{\rm opt}$, which corresponds to the optimal packing of its molecules. The membrane experiences a mechanical tension, $\Sigma_{\rm mec}$, when its area A deviates from the optimal area $A_{\rm opt}$. This mechanical tension can be expressed as

$$\Sigma_{\rm mec}(A) = K_A\,\frac{A - A_{\rm opt}}{A_{\rm opt}} \tag{14}$$

up to first order in $A - A_{\rm opt}$, which defines the area compressibility modulus K_A.

The work of stretching or compression, starting from the initial area $A = A_{\rm opt}$, defines the stretching energy

$$E_{\rm st}(A) = \int_{A_{\rm opt}}^{A} dx\,\Sigma_{\rm mec}(x) = (1/2)K_A\frac{\left(A - A_{\rm opt}\right)^2}{A_{\rm opt}}. \tag{15}$$

which may be rewritten in the form

$$E_{\rm st}(A) = A_{\rm opt}\Sigma^2_{\rm mec}(A)/(2K_A) \tag{16}$$

Compared to the term ΣA that appears in the auxiliary quantity $E^{\rm inc}_{\rm ve}(\Delta P,\Sigma)$ as given by Eq. (7), the stretching energy $E_{\rm st}(A)$ is proportional to the additional factor $\Sigma_{\rm mec}/(2K_A)$. The mechanical tension $\Sigma_{\rm mec}$ must be smaller than the tension of rupture, $\Sigma_{\rm rup}$. Therefore, the stretching energy also satisfies the inequality

$$E_{\rm st}(A) \lesssim \frac{\Sigma_{\rm rup}}{2K_{\rm A}}\,\Sigma_{\rm mec}A_{\rm opt}. \tag{17}$$

For lipid bilayers, the rupture tension $\Sigma_{\rm rup}$ is about two orders of magnitude smaller than the area compressibility modulus K_A as discussed further below in subsection 4.6.

4.2. Combined bending and stretching energy

Now, let us again consider an arbitrary vesicle shape $\mathcal{S}$. The total elastic energy of the vesicle membrane, which consists of its combined bending and stretching energy, is now equal to

$$\mathcal{E}_{\rm el}\{\mathcal{S}\} = \mathcal{E}_{\rm be}\{\mathcal{S}\} + E_{st}(\mathcal{A}\{\mathcal{S}\}) \equiv \mathcal{E}_{\rm be}\{\mathcal{S}\} + \mathcal{E}_{\rm st}\{\mathcal{S}\}. \tag{18}$$

The corresponding shape functional of the vesicle has the form

$$\mathcal{E}^{\rm com}_{\rm ve}\{\mathcal{S}\} = -\Delta P \mathcal{V}\{\mathcal{S}\} + \mathcal{E}_{\rm be}\{\mathcal{S}\} + \mathcal{E}_{\rm st}\{\mathcal{S}\} \tag{19}$$

where the superscript 'com' refers to compressible membranes and the Lagrange multiplier ΔP is used, as before, to enforce a certain prescribed vesicle volume.

4.3. Two-step minimization procedure

The minimization of the shape functional (19) can be performed in two steps:

(i) First, we minimize the shape functional (7) using the Lagrange multiplier tension Σ to enforce the membrane area A. As a result, we obtain the bending energy function

$$E_{\rm be}(V,A) = \mathcal{E}_{\rm be}\{\mathcal{S}^{\rm eq}\} \tag{20}$$

as in Eq. (11), which represents the membrane's bending energy as a function of volume V and membrane area A along a branch of (meta)stable equilibrium shapes $\mathcal{S}^{\rm eq}$. In general, we expect to find several branches of such shapes as illustrated in Fig. 4 for vanishing spontaneous curvature, $m = 0$.

(ii) Second, we minimize the combined elastic energy functional $\mathcal{E}_{\rm el} = \mathcal{E}_{\rm be} + \mathcal{E}_{\rm st}$ with respect to membrane area A for fixed volume V. Because the stretching energy is an explicit function of the membrane area, we can replace the minimization of the elastic energy functional $\mathcal{E}_{\rm el}$ by the minimization of the elastic energy function

$$E_{\rm el}(V,A) \equiv E_{\rm be}(V,A) + E_{\rm st}(A) = E_{\rm be}(V,A) + \frac{1}{2}K_A\frac{\left(A-A_{\rm opt}\right)^2}{A_{\rm opt}}. \tag{21}$$

The relation $(dE_{\rm el}(V,A)/dA)_V = 0$ then determines the equilibrium value $A = A^{\rm eq}$ of the membrane area via

$$K_A\frac{A^{\rm eq}-A_{\rm opt}}{A_{\rm opt}} = -\left(\frac{dE_{\rm be}(V,A^{\rm eq})}{dA^{\rm eq}}\right)_V. \tag{22}$$

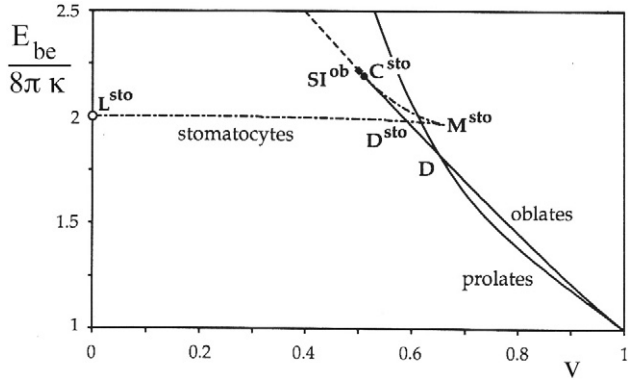

Fig. 4. Bending energy $E_{\rm be}$ as a function of reduced volume $v \equiv 6\sqrt{\pi}V/A^{3/2}$ for the spontaneous curvature model with $m = 0$ [6]. The slope $dE_{\rm be}/{\rm dv}$ is proportional to $-(dE_{\rm be}/dA)_V$.

In this way, the minimization of the combination of bending and stretching energy has been reduced to the minimization of the bending energy alone, which determines the bending energy $E_{\rm be}$ as a function of V and A.

4.4. Mechanical tension from membrane bending

The relation as given by Eq. (22) has a very simple physical interpretation. By definition, the left-hand side of Eq. (22) is equal to the mechanical tension $\Sigma_{\rm mec}$, see Eq. (14), whereas the right-hand side of this equation is equal to the Lagrange multiplier tension Σ as in Eq. (13). Therefore, the relation (22) is equivalent to

$$\Sigma_{\rm mec} = K_A\frac{A^{\rm eq}-A_{\rm opt}}{A_{\rm opt}} = -\left(\frac{dE_{\rm be}(V,A^{\rm eq})}{dA^{\rm eq}}\right)_V = \Sigma \tag{23}$$

which reveals that the Lagrange multiplier tension Σ is, in fact, identical with the mechanical tension $\Sigma_{\rm mec}$. The identity (23) is not restricted to a specific form of the bending energy but holds for any such energy, when minimized for fixed vesicle volume and fixed membrane area. An analogous equation also holds for the bilayer coupling model [26], in which the bending energy function $E_{\rm be}$ depends on the volume V, membrane area A, as well as total mean curvature $\mathcal{M} \equiv \int dA\, M$, and the partial derivative on the right-hand side of Eq. (23) has to be taken at constant volume V and constant total mean curvature $\mathcal{M}$.

4.5. Membrane stretching and compression

Inspection of relation (23) shows that the membrane is *stretched* with

$$A^{\rm eq} > A_{\rm opt} \quad \text{for} \quad \left(\frac{dE_{\rm be}(V,A^{\rm eq})}{dA^{\rm eq}}\right)_V < 0 \tag{24}$$

and that it is *compressed* with

$$A^{\rm eq} > A_{\rm opt} \quad \text{for} \quad \left(\frac{dE_{\rm be}(V,A^{\rm eq})}{dA^{\rm eq}}\right)_V < 0. \tag{25}$$

As a simple but instructive example, let us consider the case with vanishing spontaneous curvature. In this case, the reduced elastic bending energy $E_{\rm be}/\kappa$ depends only on the reduced volume v, i.e., $E_{\rm be}(V,A) = \kappa E_0(v)$ as depicted in Fig. 4 [6]. Using the relation

$$\left(\frac{dE_{\rm be}(V,A)}{dA}\right)_V = -\kappa\frac{3v}{2A}\frac{dE_0(v)}{dv} \quad (m=0) \tag{26}$$

we conclude from Fig. 4 that the vesicle membranes are compressed along the prolate and oblate branches and have an area close to the optimal area along the stomatocyte branch.

In Fig. 4, the vicinity of the spherical shape with reduced volume $v = 1$ provides an example for a branch of stable shapes close to a limit shape. Because $(dE_{\rm be}/dA)_V > 0$ along this branch, the vesicle membrane is compressed and the shape that minimizes the combined elastic energy $E_{\rm be} + E_{\rm st}$ for fixed V has the area $A^{\rm eq} < A_{\rm opt}$. However, the smallest area that the vesicle can attain for fixed V is provided by the spherical area

$$A_{\rm sp}(V) = (4\pi)^{1/3}3^{2/3}V^{2/3}, \tag{27}$$

which implies that the equilibrium value $A^{\rm eq}$ of the membrane area must satisfy the inequality

$$A^{\rm eq} \geq A_{\rm sp}(V). \tag{28}$$

Now, as we approach the spherical limit shape, the area A that minimizes $E_{\rm be} + E_{\rm st}$ for fixed V will eventually move into the unphysical region with $A < A_{\rm sp}(V)$. In such a situation, we need to replace the

smooth minimum obtained from Eq. (23) by the boundary minimum with $A^{eq} = A_{sp}(V)$.

4.6. Weakly compressible membranes

So far, the magnitude of the area compressibility modulus K_A has not been taken into account. For lipid bilayers, this material parameter, which has the dimension of a tension, is about 200 mN/m [40]. Therefore, this modulus is two orders of magnitude larger than the tension of rupture, which represents the largest mechanical tension that can be applied to the membrane. Likewise, the area compressibility modulus K_A is always much larger than the tension-like parameter combinations κ/R_{ve}^2, $\kappa m/R_{ve}$, and κm^2 where R_{ve} is the linear size of the vesicle as defined by its volume or area.

For lipid bilayers, the rupture tension Σ_{rup} is of the order of a few mN/m, which is about two orders of magnitude smaller than the area compressibility modulus K_A. Therefore, for lipid bilayers at their equilibrium area $A = A^{eq}$, the inequality (17) for the stretching energy becomes

$$E_{st}(A^{eq}) \lesssim 10^{-2}\, \Sigma_{mec} A_{opt}. \tag{29}$$

Thus, for these membranes, the stretching energy is smaller than $\Sigma_{mec} A_{opt}$ by at least two orders of magnitude.

Inspection of the combined bending and stretching energy $E_{be} + E_{st}$ as given by Eq. (21) shows that the membrane area has the equilibrium value

$$A^{eq} \approx A_{opt} \quad \text{in the limit of large} \quad K_A. \tag{30}$$

Therefore, in this limit, we may expand the bending energy E_{be} around $A = A_{opt}$ which leads to

$$E_{be}(V,A) \approx E_{opt}^{(0)} + \Delta A\, E_{opt}^{(1)} + \frac{1}{2}(\Delta A)^2 E_{opt}^{(2)} \tag{31}$$

up to second order in

$$\Delta A \equiv A - A_{opt} \tag{32}$$

with the partial derivatives

$$E_{opt}^{(n)} \equiv \frac{\partial^n E_{be}}{\partial A^n}\Big|_{A_{opt}}. \tag{33}$$

If we insert this expansion into expression (21) for the combined bending and stretching energy and minimize the latter energy with respect to area A, we obtain the asymptotic equality

$$E_{opt}^{(1)} + \left(A^{eq} - A_{opt}\right)\left[E_{opt}^{(2)} + \frac{K_A}{A_{opt}}\right] \approx 0 \tag{34}$$

which implies the area dilation

$$A^{eq} - A_{opt} \approx -A_{opt}\frac{E_{opt}^{(1)}}{K_A}\left[1 - \frac{A_{opt}E_{opt}^{(2)}}{K_A}\right] \tag{35}$$

up to second order in $1/K_A$. Likewise, the stretching energy becomes

$$E_{st}(A^{eq}) = \frac{1}{2}K_A\,\frac{\left(A^{eq} - A_{opt}\right)^2}{A_{opt}} \approx A_{opt}\left[E_{opt}^{(1)}\right]^2/(2K_A) \tag{36}$$

up to first order in $1/K_A$.

5. Mechanical tensions for simple vesicle shapes

In this section, a couple of examples are discussed for which one can explicitly calculate the mechanical tension Σ_{mec} using the spontaneous curvature model. In the first two examples, the scale for the mechanical tension is provided by the spontaneous tension $\sigma = 2\kappa m^2$, whereas, in the last two examples, the mechanical tension is much smaller than the spontaneous tension.

5.1. Spherical vesicles

First, consider the simplest vesicle morphology as provided by spherical shapes. The mean curvature M_{sp} of the sphere satisfies the relation

$$\Delta P = 2\left(\Sigma + 2\kappa m^2\right)M_{sp} - 4\kappa m M_{sp}^2 \tag{37}$$

as follows by minimizing the shape functional (6) for the bending energy (2). Because the relation (37) is obtained when the shape is displaced in the direction of its normal vectors, this relation represents the normal stress balance for each membrane segment. Such a spherical shape is stable provided [41,6,38]

$$\Delta P > P_{sp}^* \equiv 4\kappa M_{sp}^2\left(m - 3M_{sp}\right). \tag{38}$$

At the critical pressure $P = P_{sp}^*$, the spherical shape loses its stability and starts to transform into a prolate or oblate shape, where the prolate shape has the lowest bending energy for small m/M_{sp}-values whereas the oblate shape represents the lower energy shape for sufficiently large negative values of m/M_{sp}, see Fig. 10 in [6].[1]

It is therefore useful to rewrite the normal stress balance (37) in the form

$$\Sigma_{mec} = \Sigma = \Sigma_{sp}^* + \frac{\Delta P - P_{sp}^*}{2M_{sp}} \tag{39}$$

with the threshold tension

$$\Sigma_{sp}^* \equiv -2\kappa\left(m^2 - 2mM_{sp} + 3M_{sp}^2\right). \tag{40}$$

The stability condition $\Delta P > P_{sp}^*$ then implies that stable spheres are characterized by $\Sigma_{mec} > \Sigma_{sp}^*$.

The reduced threshold tension Σ_{sp}^*/κ depends on the mean curvature M_{sp} of the spherical vesicle, which is taken to be positive here, and on the spontaneous curvature m, which may attain positive or negative values. It is then useful to consider the straight lines

$$M_{sp} = \alpha m \quad \text{with} \quad \alpha \neq 0 \tag{41}$$

within the $(m, M_{sp} > 0)$ half plane. The threshold tension now becomes

$$\Sigma_{sp}^* = -2\kappa m^2\left(3\alpha^2 - 2\alpha + 1\right) = -\sigma\left(3\alpha^2 - 2\alpha + 1\right) \tag{42}$$

which implies, together with Eq. (40), that

$$\Sigma_{sp}^* < 0 \quad \text{for all} \quad m. \tag{43}$$

A vesicle with $M_{sp} = m$ and $\alpha = 1$, for example, is characterized by the threshold tension $\Sigma_{sp}^* = -4\kappa m^2 = -2\sigma$. Furthermore, the smallest absolute value $|\Sigma_{sp}^*|$ corresponding to the smallest compression of the vesicle membrane at the bifurcation point is obtained for $\alpha = 1/3$, which leads to $\Sigma_{sp}^* = -\frac{4}{3}\kappa m^2 = -\frac{2}{3}\sigma$.

5.2. Small spheres connected to large sphere

Next, consider a small spherical bud connected to a large sphere by a small membrane neck. The small and the large spheres have the radii R_{ss}

[1] Fig. 10 in Ref. [6] first appeared in the diploma thesis of K. Berndl [42].

and R_{ls}, respectively, both of which are always taken to be positive. The sign convention for the curvature implies that the mean curvature $M_{ls} = 1/R_{ls}$ of the large sphere is always positive as well whereas the mean curvature $M_{ss} = \pm 1/R_{ss}$ of the small sphere is positive for an out-bud as in Fig. 5(a) and negative for an in-bud as in Fig. 5(b).

The out-bud shape shown in Fig. 5(a) can arise from the osmotic deflation of a pear-like vesicle provided the area of this vesicle membrane satisfies $A \geq 8\pi/m^2$ where the equality sign corresponds to $R_{ss} = R_{ls}$. The equality with $A = 8\pi/m^2$ corresponds to the reduced volume $v = 6\sqrt{\pi}V/A^{3/2} = 1/\sqrt{2} \approx 0.71$ and the reduced spontaneous curvature $c_0 \equiv 2m(A/4\pi)^{1/2} = 2^{3/2} \simeq 2.83$, which determines the end point of the line L^{pear} in Fig. 10 of Ref. [6]. The in-bud shape in Fig. 5(b) can arise from the osmotic deflation of a stomatocyte without any restriction on its membrane area. An alternative process, by which one can obtain the shapes in Fig. 5(a) and (b) as limit shapes from smoothly curved vesicle shapes, is by increasing the positive spontaneous curvature of pear-like vesicles and decreasing the negative spontaneous curvature of stomatocytes, see the lines denoted by L^{pear} and L^{sto} in Fig. 10 of Ref. [6]. When the ideal necks arise as limiting shapes of wider necks, they satisfy the ideal neck condition [42,6,38]

$$M_{ls} + M_{ss} = 2m, \tag{44}$$

which implies that positive spontaneous curvatures $m > 0$ always lead to out-buds whereas negative spontaneous curvatures $m < 0$ always lead to in-buds. The ideal neck condition (44) has been used to estimate the spontaneous curvature m induced by the adsorption of biotinylated DNA bound to membrane-anchored avidin [37].

One may also consider an ideal neck and ask under what conditions this neck is locally stable. One then finds the curvature inequality [43]

$$M_{ls} + M_{ss} < 2m \quad \text{for locally stable out}-\text{buds} \quad (m>0) \tag{45}$$

as in Fig. 5(a) and the inequality [44]

$$M_{ls} + M_{ss} > 2m \quad \text{for locally stable in}-\text{buds} \quad (m<0) \tag{46}$$

as in Fig. 5(b), the latter being equivalent to $-M_{ls} + |M_{ss}| < 2|m|$.

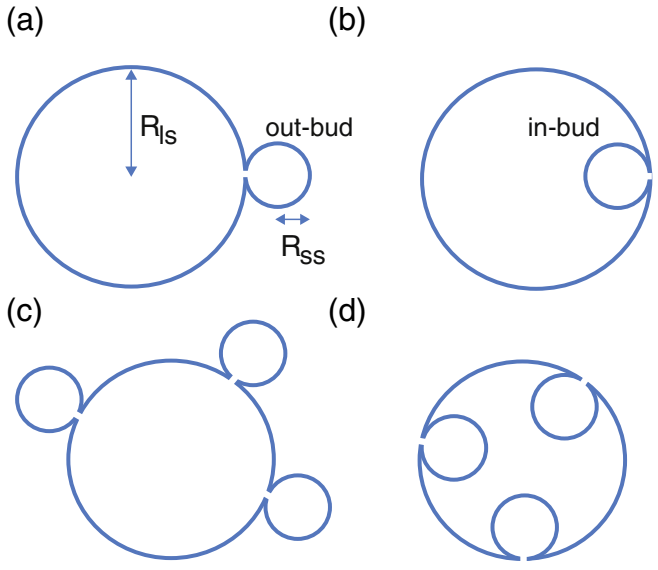

Fig. 5. Small spherical buds connected to a large spherical vesicle by narrow necks: (a,c) Out-buds that protrude into the exterior compartment can be formed for $m > 0$, whereas (b,d) In-buds that protrude into the interior compartment imply $m < 0$. The large vesicle has the radius R_{ls}; when the buds form as limit shapes, the out-buds have the radius $R_{ss} = R_{ls}/(2mR_{ls} - 1)$ and the in-buds have the radius $R_{ss} = R_{ls}/(1 - 2mR_{ls})$.

The two mean curvatures M_{ls} and M_{ss} satisfy the normal stress balance relations

$$\Delta P = 2\left(\Sigma + 2\kappa m^2\right)M_{sp} - 4\kappa m M_{sp}^2 \quad \text{with} \quad M_{sp} = M_{ls} \text{ or } M_{ss}. \tag{47}$$

Eliminating the pressure difference from these two equations and inserting the ideal neck condition, the mechanical tension is found to satisfy the simple relation

$$\Sigma_{mec} = \Sigma = 2\kappa m^2 = \sigma, \tag{48}$$

which is valid for the limit shapes of both out- and in-buds. Thus, for this vesicle morphology, the scale for the mechanical tension is again provided by the spontaneous tension σ, but, compared to the threshold tension Σ_{sp}^* for spherical vesicles as discussed in the previous subsection, the mechanical tension now has the opposite sign and acts to stretch the membrane.

The relation $\Sigma = 2\kappa m^2$ was first obtained from numerical solutions for axially symmetric vesicle shapes [6]. The derivation presented here implies that the relation (48) also applies to limit shapes consisting of a large sphere and an arbitrary number of small spheres, all connected to the large sphere by small membrane necks, see Fig. 5(c,d). Because of the ideal neck condition, all small spheres must have the same mean curvature $M_{ss} = 2m - M_{ls}$, which implies that all small spheres are either out- or in-buds and that they all have the same radius R_{ss}. In general, morphologies as in Fig. 5(c,d) can arise from nonuniform perturbations of the membrane and may represent limit shapes with $M_{ls} + M_{ss} = 2m$ or locally stable shapes with $M_{ls} + M_{ss} > 2m$ or $M_{ls} + M_{ss} < 2m$ for out- and in-buds, respectively.

Starting from the shapes in Fig. 5(c,d), one can construct somewhat different morphologies by detaching one small sphere from the large sphere and reattaching it, via an ideal neck, to one of the other small spheres. Because the ideal necks have vanishing bending energy [6], this 'cut and paste' operation does not change the bending energy of the vesicle membrane but the resulting shapes exhibit two different ideal necks: ss–ls-necks between a small sphere and the large sphere as well as ss–ss-necks between two identical small spheres. Both types of necks can, in fact, be locally stable at the same time. Using the curvature inequalities in Eqs. (45) and (46) for both types of ideal necks, one concludes that both ss–ls-necks and ss–ss-necks are locally stable for out-buds with $M_{ss} \leq m$ and for in-buds with $M_{ss} \geq m$, the latter inequality being equivalent to $|m| \geq |M_{ss}|$. Thus, ss–ls-necks and ss–ss-necks can coexist in both cases for sufficiently large absolute values of the spontaneous curvature.

5.3. Cylindrical tubules connected to large sphere

Another example, for which the mechanical tension can be calculated explicitly, is provided by cylindrical tubules that are connected to a large sphere, see Fig. 6(a,b). If the tubule and the sphere are in mechanical equilibrium, we have three stress balance conditions. First, the mean curvature M_{sp} of the sphere again satisfies the relation (37). Second, the normal stress balance for the cylindrical tube has the form

$$\Delta P = 2\left(\Sigma + 2\kappa m^2\right)M_{cy} - 4\kappa M_{cy}^3 \tag{49}$$

whereas the tangential stress balance along the tube is described by

$$\Delta P = 4\left(\Sigma + 2\kappa m^2\right)M_{cy} - 16\kappa m M_{cy}^2 + 8\kappa M_{cy}^3 \tag{50}$$

Eliminating the pressure difference ΔP and the tension Σ from the three Eqs. (37), (49), and (50), one obtains the mean curvature [18,19]

$$M_{cy} \approx m - \frac{1}{4}M_{ls} \quad \text{for small} \quad M_{ls}/|m| \tag{51}$$

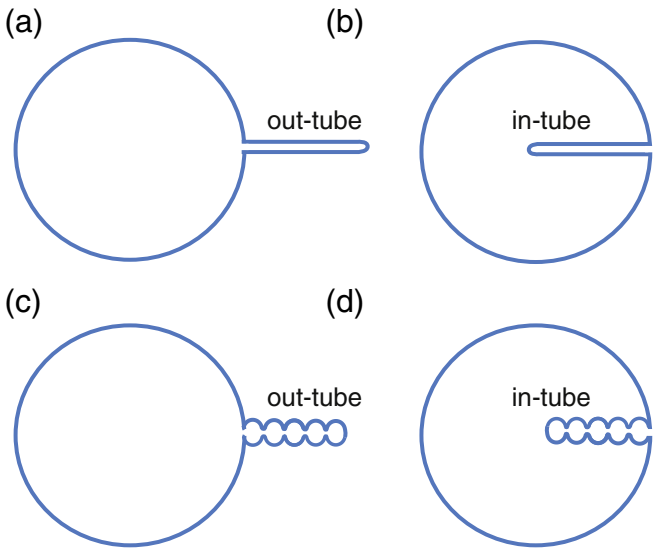

Fig. 6. Membrane nanotubes emanating from a large spherical vesicle: (a,b) Cylindrical in- and out-tubes; and (c,d) Necklace-like in- and out-tubes consisting of a string of small spheres.

of the cylindrical tube and the mechanical tension

$$\Sigma_{\rm mec} = \Sigma \approx \kappa m M_{\rm ls} \quad \text{for small} \quad M_{\rm ls}/|m| \tag{52}$$

within the whole membrane.

If we were able to measure the tube radius $R_{\rm cy}$, we could also determine the spontaneous curvature via

$$m \approx M_{\rm cy} + \frac{1}{4} M_{\rm ls} = \pm \frac{1}{2R_{\rm cy}} + \frac{1}{4R_{\rm ls}} \tag{53}$$

where the plus and minus signs apply to the out- and in-tubes as shown in Fig. 6(a,b), respectively. Linear stability analysis implies that cylindrical in-tubes are stable whereas cylindrical out-tubes are unstable and transform into necklace-like out-tubes, see Fig. 6(c,d) and the next subsection [19]. However, because the two shapes can be continuously transformed into each other via unduloids that have the same area, the same mean curvature, and the same bending energy, both cylindrical and necklace-like morphologies may coexist in the same vesicle.

5.4. Necklace-like tubules connected to large sphere

Now, as a last example, let us consider the necklace-like tubules as depicted in Fig. 6(c,d). The mean curvatures of the large spherical 'mother' vesicle and of the small spheres within the necklace-like tubules again satisfy the two relations in Eq. (47). Furthermore, the tangential stress balance along the necklace-like tube now has the form

$$\Delta P = 3\left(\Sigma + 2\kappa m^2\right) M_{\rm ss} - 12\kappa m M_{\rm ss}^2 + 6\kappa M_{\rm ss}^3. \tag{54}$$

Eliminating again ΔP and Σ from the three relations in Eqs. (47) and (54), we obtain the mean curvature

$$M_{\rm ss} \approx m - \frac{1}{3} M_{\rm ls} \quad \text{for small} \quad M_{\rm ls}/|m| \tag{55}$$

of the small spheres and the mechanical tension

$$\Sigma_{\rm mec} = \Sigma \approx \frac{4}{3} \kappa m M_{\rm ls} \quad \text{for small} \quad M_{\rm ls}/|m| \tag{56}$$

within the whole membrane for both out- and in-tubes.

Neighboring spheres within the necklace now satisfy the perturbed neck condition

$$M_{\rm ss} + M_{\rm ss} \approx 2m - \frac{2}{3} M_{\rm ls} \tag{57}$$

which becomes identical to the ideal neck condition (44) in the limit of vanishing $M_{\rm ls}$ corresponding to a very large sphere.[2] Because $M_{\rm ss} < m$, necklace-like out-tubes can be connected to the large sphere by an ideal ss-ls-neck.

If we were able to measure the radii $R_{\rm ss}$ of the small spheres, we could determine the spontaneous curvature also via

$$m \approx M_{\rm ss} + \frac{1}{3} M_{\rm ls} = \pm \frac{1}{R_{\rm ss}} + \frac{1}{3R_{\rm ls}} \tag{58}$$

where the plus and minus signs apply to out-tubes and in-tubes as in Fig. 6(c) and (d), respectively.

6. Summary and outlook

The mechanical tension $\Sigma_{\rm mec}$ has been determined by minimizing the combined bending and stretching energy with respect to membrane area for fixed vesicle volume. This minimization leads to the relation (23) which shows that the mechanical tension $\Sigma_{\rm mec}$ is identical with the Lagrange multiplier tension Σ that has been adjusted in the minimization of the bending energy to enforce a certain, prescribed equilibrium value of the membrane area.

The identity of the mechanical tension with the Lagrange multiplier tension has then be used in Section 5 to determine the mechanical tension for a variety of simple shapes.

For a spherical vesicle close to the prolate/oblate instability, the mechanical tension $\Sigma_{\rm mec}$ is negative and its absolute value is of the order of the spontaneous tension $2\kappa m^2$, see Eq. (42). For limit shapes with spherical in- and out-buds connected to a larger sphere as in Fig. 5(a,b), the mechanical tension is positive and equal to the spontaneous tension, see Eq. (48). On the other hand, for cylindrical or necklace-like tubes connected to a large spherical vesicle, the mechanical tension is negative and much smaller than the spontaneous tension, see Eqs. (52) and (56).

The same analysis can be applied to more complex vesicle geometries. One example is provided by vesicles enclosing two aqueous droplets as shown in Fig. 7. In this case, the vesicle membrane consists of two segments, the $\alpha\gamma$ segment between the α droplet and the external γ phase as well as the $\beta\gamma$ segment between the β droplet and the γ phase. The two segments form a three-phase contact line with the $\alpha\beta$ interface between the two droplets. The force balance along this contact line involves the total membrane tensions [18,19]

$$\hat{\Sigma}_q \equiv \Sigma_q + \sigma_q \quad \text{with} \quad q = \alpha\gamma \text{ or } \beta\gamma \tag{59}$$

of the two membrane segments with the mechanical tensions $\Sigma_{{\rm mec},q} \equiv \Sigma_q$. If the segment q forms nanotubes, the spontaneous tension σ_q is large compared to the mechanical tension $\Sigma_{{\rm mec},q}$ and one can determine the spontaneous curvature of the q-segment from the measured contact angles, see Fig. 7.

The two-droplet geometry in Fig. 7 involves an extrinsic tension scale as provided by the interfacial tension $\Sigma_{\alpha\beta}$ of the interface between the two droplets. Along the contact line, the latter tension must be balanced by the tensions $\hat{\Sigma}_{\alpha\gamma}$ and $\hat{\Sigma}_{\beta\gamma}$ of the two membrane

[2] The correction terms in Ref. [18] have different prefactors because, in the latter reference, the ideal neck condition has been used, corresponding to Eq. (57) without the correction term $-\frac{2}{3}M_{\rm ls}$.

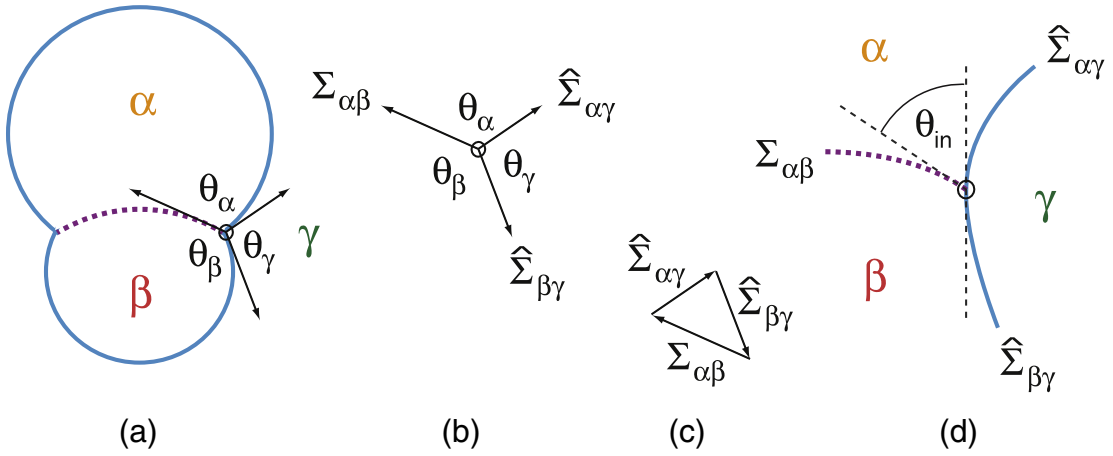

Fig. 7. Geometry of a large vesicle enclosing two aqueous droplets: (a) The vesicle membrane (solid blue line) separates the two interior aqueous phases α and β from the exterior aqueous phase γ. This membrane consists of two spherical segments, one segment in contact with the α phase and another segment in contact with the β phase. The $\alpha\beta$ interface (broken purple line) and the two membrane segments meet along the contact line, which defines the three effective contact angles θ_α, θ_β, and θ_γ; (b) Mechanical equilibrium at the contact line implies that the interfacial tension $\Sigma_{\alpha\beta}$ balances the two membrane tensions $\hat{\Sigma}_{\alpha\gamma}$ and $\hat{\Sigma}_{\beta\gamma}$; (c) Triangle formed by the three tensions $\Sigma_{\alpha\beta}$, $\hat{\Sigma}_{\alpha\gamma}$, and $\hat{\Sigma}_{\beta\gamma}$; and (d) Intrinsic contact angle $\theta_{\rm in}$ when the membrane is viewed with nanoscopic resolution [45].

segments. If the $\alpha\gamma$ segment forms tubules, the force balance implies [19,30]

$$\hat{\Sigma}_{\beta\gamma} = \Sigma_{\beta\gamma} + \sigma_{\beta\gamma} \approx \sigma_{\alpha\gamma} + \Sigma_{\alpha\beta}\,\frac{\sin\theta_\alpha - \sin\theta_\beta}{\sin\theta_\gamma} \tag{60}$$

which can be used to determine the spontaneous tension $\sigma_{\alpha\gamma}$. The three (effective) contact angles θ_α, θ_β, and θ_γ are defined in Fig. 7(a,b); the trigonometric term $(\sin\theta_\alpha - \sin\theta_\beta)/\sin\theta_\gamma$ is equal to $\cos(\theta_{\rm in})$ with the intrinsic contact angle $\theta_{\rm in}$ as defined in Fig. 7(d) [45]. The relation (60) implies that the $\beta\gamma$ segment can adapt its mechanical tension $\Sigma_{{\rm mec},\beta\gamma} = \Sigma_{\beta\gamma}$ in order to balance the other two tensions along the contact line.

Another vesicle geometry that involves an extrinsic tension scale is provided by vesicles adhering to a solid surface as in Fig. 8. In this case, the extrinsic tension scale corresponds to the adhesive strength W, which represents the adhesion free energy per unit area. Theoretical considerations predict that the vesicle will unbind from the surface by the formation of tubules, see Fig. 8(b,c), as soon as the spontaneous tension $\sigma = 2\kappa m^2$ of the membrane exceeds the critical value $\sigma = \sigma^* = |W|$, i.e., as soon as σ exceeds the absolute value $|W|$ of the adhesive strength [30]. The variation of the spontaneous curvature can be probed experimentally by changing the concentration of adsorbate particles in the interior or exterior aqueous compartment. In this way, one can estimate the critical value of the spontaneous tension and, thus, of the spontaneous curvature if one knows the adhesive strength W and vice versa.

Finally, a few remarks about an aspect that I did not address in the main body of this paper, namely possible effects of thermally-excited shape fluctuations on the membrane tension. First, it is important to note that the mechanical tension as determined in molecular dynamics simulations [10] includes all of these fluctuation effects. Second, for small or 'harmonic' fluctuations around an equilibrium shape of the vesicle, the vesicle membrane experiences an 'effective tension', which can be identified with the Lagrange multiplier tension, provided the fluctuation modes break the symmetry of the equilibrium shape [46]. The identity between the Lagrange multiplier tension and the mechanical tension as derived in the present paper implies that the symmetry-breaking modes are, in fact, governed by the mechanical tension within the vesicle membrane.

The spectrum of thermally-excited shape fluctuations can also be determined by molecular dynamics simulations [11]. In the presence of membrane tension, the fluctuation spectrum should scale as $1/k^2$ for small wavenumber k, and the coefficient of this k-dependence also defines a tension, the fluctuation tension. One interesting and open question is the relation between this fluctuation tension and the mechanical tension. In our original molecular dynamics simulations of the fluctuation spectrum, we implicitly assumed that the two tensions can be identified. On the one hand, subsequent molecular dynamics simulations found small differences between the numerical values of the two tensions [47–49]. On the other hand, symmetry arguments and simulations of '1-dimensional membranes', which are equivalent to semiflexible polymers or wormlike chains [50], seem to support the identity of fluctuation and mechanical tension [51,52]. Because the molecular dynamics simulations in [47–49] were necessarily restricted to certain ranges of membrane areas, it is possible that the small differences between the two tensions as found in these simulations arise from finite-size effects. Thus, one would like to study these effects in a systematic manner

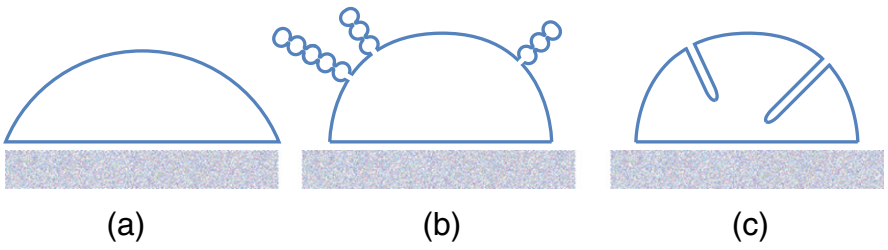

Fig. 8. Vesicle adhering to a solid surface: (a) If the vesicle membrane has a small spontaneous curvature, the adhering vesicle forms a spherical cap, the geometry of which reflects its volume-to-area ratio; (b,c) Membrane binding of proteins or nanoparticles that generate a large positive or negative spontaneous curvature m: If the absolute value $|m|$ exceeds a certain threshold value, the vesicle starts to reduce its contact area with the solid surface and store the resulting excess area in necklace-like out-tubes for $m > 0$ as in (b) and in cylindrical in-tubes for $m < 0$ as in (c). In both cases, the tubulation process will continue until the contact area disappears and the vesicle unbinds from the solid surface [30]. The free energy difference between necklace-like and cylindrical tubes is quite small, which implies peristaltic shape fluctuations that connect the two tube morphologies.

by increasing the size of the membrane patches. However, larger membrane patches are less stable against rupture or pore formation [15,53], which implies that the range of mechanical tensions that can be explored in the simulations shrinks as one increases the size of the membranes. So, even today, the notion of membrane tension continues to provide us with both conceptual and computational challenges.

Acknowledgments

I thank all my collaborators for fruitful and enjoyable interactions and Jaime Agudo for stimulating discussions about membrane compressibility and neck conditions.

References

[1] Lipowsky R, Leibler S. Unbinding transitions of interacting membranes. Phys Rev Lett 1986;56:2541–4.
[2] Mutz M, Helfrich W. Unbinding transition of a biological model membrane. Phys Rev Lett 1989;62:2881–4.
[3] Helfrich W. Elastic properties of lipid bilayers: theory and possible experiments. Z Naturforsch 1973;28c:693–703.
[4] Deuling H, Helfrich W. The curvature elasticity of fluid membranes: a catalogue of vesicle shapes. J Phys 1976;37:1335–45.
[5] Berndl K, Käs J, Lipowsky R, Sackmann E, Seifert U. Shape transformations of giant vesicles: extreme sensitivity to bilayer asymmetry. Europhys Lett 1990;13:659–64.
[6] Seifert U, Berndl K, Lipowsky R. Shape transformations of vesicles: phase diagram for spontaneous curvature and bilayer coupling model. Phys Rev A 1991;44:1182–202.
[7] Lipowsky R. The conformation of membranes. Nature 1991;349:475–81.
[8] Miao L, Seifert U, Wortis M, Döbereiner H-G. Budding transitions of fluid-bilayer vesicles: the effect of area-difference elasticity. Phys Rev E 1994;49:5389–407.
[9] Döberreiner H-G, Evans E, Kraus M, Seifert U, Wortis M. Mapping vesicle shapes into the phase diagram: a comparison of experiment and theory. Phys Rev E 1997;55(4):4458–74.
[10] Goetz R, Lipowsky R. Computer simulations of bilayer membranes: self-assembly and interfacial tension. J Chem Phys 1998;108:7397–409.
[11] Goetz R, Gompper G, Lipowsky R. Mobility and elasticity of self-assembled membranes. Phys Rev Lett 1999;82:221–4.
[12] Ayton G, Voth GA. Bridging microscopic and mesoscopic simulations of lipid bilayers. Biophys J 2002;83:3357–70.
[13] Shillcock JC, Lipowsky R. Equilibrium structure and lateral stress distribution of amphiphilic bilayers from dissipative particle dynamics simulations. J Chem Phys 2002;117:5048–61.
[14] Srinivas G, Discher DE, Klein ML. Self-assembly and properties of diblock copolymers by coarse-grain molecular dynamics. Nat Mater 2004;3:638–44.
[15] Tolpekina TV, den Otter WK, Briels WJ. Simulations of stable pores in membranes: system size dependence and line tension. J Chem Phys 2004;121:8014–20.
[16] Grafmüller A, Shillcock JC, Lipowsky R. The fusion of membranes and vesicles — Pathway and energy barriers form dissipative particle dynamics. Biophys J 2009;96:2658–75.
[17] Hu M, Briguglio JJ, Deserno M. Determining the Gaussian curvature modulus of lipid membranes in simulations. Biophys J 2012;102:1403–10.
[18] Li Y, Lipowsky R, Dimova R. Membrane nanotubes induced by aqueous phase separation and stabilized by spontaneous curvature. Proc Natl Acad Sci U S A 2011;108:4731–6.
[19] Lipowsky R. Spontaneous tubulation of membranes and vesicles reveals membrane tension generated by spontaneous curvature. Faraday Discuss 2013;161:305–31.
[20] Lipowsky R, Grotehans S. Hydration versus protrusion forces between lipid bilayers. Europhys Lett 1993;23:599–604.
[21] Brannigan G, Brown FLH. A consistent model for thermal fluctuations and protein-induced deformations in lipid bilayers. Biophys J 2006;90:1501–20.
[22] Bancroft WD. The theory of emulsification, V. J Phys Chem 1913;17:501–19.
[23] Frank FC. Liquid crystals I: on the theory of liquid crystals. Discuss Faraday Soc 1958;25:19–28.
[24] Mitov M. Third and fourth order curvature elasticity of lipid bilayers. C R Acad Bulg Sci 1978;31:513–5.
[25] Evans E. Bending resistance and chemically induced moments in membrane bilayers. Biophys J 1974;14:923–31.
[26] Svetina S, Zeks B. Membrane bending energy and shape determination of phospholipid vesicles and red blood cells. Eur Biophys J 1989;17:101–11.
[27] Lipowsky R. From membranes to membrane machines. In: Reguera D, Rubi JM, Vilar JMB, editors. Statistical mechanics of biocomplexity, Lecture Notes in Physics. Berlin: Springer; 1999. p. 1–23.
[28] Bruckner RJ, Mansy SS, Ricardo A, Mahadevan L, Szostak JW. Flip-flop-induced relaxation of bending energy: implications for membrane remodeling. Biophys J 2009;97:3113–22.
[29] Lipowsky R, Döbereiner HG. Vesicles in contact with nanoparticles and colloids. Europhys Lett 1998;43:219–25.
[30] Lipowsky R. Remodelling of membrane compartments: some consequences of membrane fluidity. Biol Chem 2014;395:253–74.
[31] Klasczyk B, Knecht V, Lipowsky R, Dimova R. Interactions of alkali metal chlorides with phosphatidylcholine vesicles. Langmuir 2010;26:18951–8.
[32] Arouni A, Kiessling V, Tamm L, Dathe M, Blume A. Morphological changes induced by the action of antimicrobial peptides on supported lipid bilayers. J Phys Chem 2011;115:158–67.
[33] Peter BJ, Kent HM, Mills IG, Vallis Y, Butler PJG, Evans PR, et al. BAR domains as sensors of membrane curvature: the amphiphysin BAR structure. Science 2004;303:495–9.
[34] McMahon HT, Gallop JL. Membrane curvature and mechanisms of dynamic cell membrane remodelling. Nature 2005;438:590–6.
[35] Rózycki B, Lipowsky R. Spontaneous curvature of bilayer membranes; 2014 (in preparation).
[36] Döbereiner HG, Selchow O, Lipowsky R. Spontaneous curvature of asymmetric bilayer membranes. Eur Biophys J 1999;28:174–8.
[37] Nikolov V, Lipowsky R, Dimova R. Behavior of giant vesicles with anchored DNA molecules. Biophys J 2007;92:4356–68.
[38] Miao L, Fourcade B, Rao M, Wortis M, Zia R. Equilibrium budding and vesiculation in the curvature model of fluid lipid vesicles. Phys Rev A 1991;43:6843–56.
[39] Seifert U. Configurations of membranes and vesicles. Adv Phys 1997;46:13–137.
[40] Evans E, Needham D. Physical properties of surfactant bilayer membranes: thermal transitions, elasticity, rigidity, cohesion, and colloidal interactions. J Phys Chem 1987;91:4219–28.
[41] Ou-Yang Z-C, Helfrich W. Bending energy of vesicle membranes: general expressions for the first, second and third variation of the shape energy and applications to spheres and cylinders. Phys Rev A 1989;39:5280–8.
[42] Berndl K. Formen von Vesikeln. [Diploma thesis] University of Munich; 1990.
[43] Fourcade B, Miao L, Rao M, Wortis M, Zia R. Scaling analysis of narrow necks in curvature models of fluid lipid-bilayer vesicles. Phys Rev E 1994;49:5276–86.
[44] R. Lipowsky, unpublished.
[45] Kusumaatmaja H, Li Y, Dimova R, Lipowsky R. Intrinsic contact angle of aqueous phases at membranes and vesicles. Phys Rev Lett 2009;103:238103.
[46] Seifert U. The concept of effective tension for fluctuating vesicles. Z Physik B 1995;97:299–309.
[47] Imparato A, Shillcock J, Lipowsky R. Shape fluctuations and elastic properties of two-component bilayer membranes. Europhys Lett 2004;69:650–6.
[48] Imparato A. Surface tension in bilayer membranes with fixed projected area. J Chem Phys 2006;124:154714.
[49] Stecki J. Size dependence, stability, and the transition to buckling in model reverse bilayers. J Chem Phys 2006;125:154902.
[50] Gutjahr P, Lipowsky R, Kierfeld J. Persistence length of semiflexible polymers and bending rigidity renormalization. Europhys Lett 2006;76:994–1000.
[51] Schmid F. Are stress-free membranes really “tensionless”? EPL 2011;95:28008.
[52] Farago O. Mechanical surface tension governs membrane thermal fluctuations. Phys Rev E 2011;84:051914.
[53] Gao L, Shillcock J, Lipowsky R. Improved dissipative particle dynamics simulations of lipid bilayers. J Chem Phys 2007;126:015101.